

where  $x_3$ ,  $y_3$  are the displacements (in centimeters) of the sulfur atom normal to the internuclear axis;  $z_1$ ,  $z_3$  are the displacements of the left and right sulfur atom along the internuclear axis;  $m_c$ ,  $m_s$  are the absolute masses of the sulfur and carbon atoms; and  $z_1^0 - z_2^0$  is the equilibrium carbon-sulfur distance.  $Q_2$  and  $Q_3$  are the normal coordinates of the corresponding modes. The numerical values of  $U_{22}''$  and  $U_{33}''$  in terms of these displacements coordinates are then  $-0.5 \times 10^5$  and  $-6 \times 10^5$  (in dyne  $\text{cm}^{-1}$ ). It is seen that these quantities are of the order of magnitude of *intramolecular bending*

and stretching constants,<sup>28</sup> respectively. Therefore, the neglect of the term  $V_{ii}U_1'$  is not permitted.

*Neglect the Term  $U_{ii}''$  of Eq. (3)*

Then  $U_1' \approx 16\pi^4 c^4 \nu_1^2 \nu_2 \Delta \nu_i / 3V_{ii}$ . For  $\nu_2$  with  $\Delta \nu_2 = 2.8 \text{ cm}^{-1}$ , it follows that  $U_1' \approx 0.9 \times 10^6 \text{ g}^{\frac{1}{2}} \cdot \text{cm} \text{ sec}^{-2}$ . However, from  $\nu_3$  with  $\Delta \nu_3 = 8.0 \text{ cm}^{-1}$ , it follows that  $U_1' \approx -10^6$ . Therefore, neglect of the term  $U_{ii}''$  is not permitted.

<sup>28</sup> See Ref. 5, p. 193.

## Simultaneous Determination of $f$ Values and Vapor Pressures from Optical Absorption Measurements\*†

PHILIP A. RICE‡ AND DAVID V. RAGONE§

*Department of Chemical and Metallurgical Engineering, University of Michigan, Ann Arbor, Michigan*

(Received 25 August 1964)

A method for determining both the  $f$  value of an absorption line and the vapor pressure of the absorbing atoms exclusively from optical absorption measurements is defined and discussed. The method depends on making absorption measurements in two regions. The first is at low optical densities, where absorption is linearly proportional to optical density. The second is at higher densities, where the center of the line is fully absorbed and the absorption is proportional to the square root of the optical density. A method for extrapolating measurements from one region to the other is also required. This is accomplished by maintaining a pure liquid in equilibrium with the absorbing vapor species over a temperature range. The method takes into account the effects of collision broadening. Measurements were made on the 3067-Å bismuth line.

### INTRODUCTION

THE  $f$  values associated with the electronic transitions of an element are often determined by measuring the absorption of the appropriate spectral lines of the element at known optical densities. This requires knowledge of vapor density, i.e., vapor pressure, during the absorption measurement. In this paper a method is developed by which the  $f$  value of a line can be determined directly from optical absorption measurements alone if these measurements can be made on vapor in equilibrium with a pure liquid over a large enough range of optical densities. The vapor pressures need not be known, although the functional relationship between vapor pressure and temperature (Clapeyron equation) is used. Optical absorption

measurements are made in the low optical density regions, where the absorption is proportional to the optical density, and in high density regions, where the absorption is proportional to the square root of the density. An extrapolation of the absorption values from one region into the other using the Clapeyron equation allows the optical density to be determined.

### SYMBOLS AND NOMENCLATURE

$A$	area under absorption curve in arbitrary units
	$= \int_0^\infty (I_0 - I_\omega) d\omega$
$B$	a constant $= \Delta C_P / R$
$b$	$b_n + b_s + b_c =$ dispersion half-breadth
$b_s$	self-collision half-breadth
	$= (\sigma_s^2 N / \pi c) (4\pi RT / M_1)^{\frac{1}{2}}$
$b_c$	collision half-breadth (due to inert gas)
	$= (\sigma_I^2 N_I / \pi c) \{ 2\pi RT [(1/M_1) + (1/M_2)] \}^{\frac{1}{2}}$
$b_n$	natural half-breadth $= 1 / (4\pi c\tau)$
$b_D$	Doppler half-breadth $= (2RT \ln 2 / M_1 c^2)^{\frac{1}{2}} \omega_0$
$c$	speed of light
$\Delta C_P$	difference in heat capacity between vapor species and liquid

\* Supported in part by U.S. Atomic Energy Commission under Contract AT(11-1)-543.

† Taken in part from the dissertation of Philip A. Rice, submitted in partial fulfillment of the requirements for the degree of Doctor of Philosophy at the University of Michigan, Ann Arbor, Michigan.

‡ Present address: Analytic Services, Inc., Bailey's Crossroads, Virginia.

§ Present address: General Atomic Division of General Dynamics Corporation, John Jay Hopkins Laboratory For Pure and Applied Science, San Diego, California.

$C_I$	a constant $= (\sigma_I^2/\pi ck) \{2\pi R[(1/M_1) + (1/M_2)]\}^{\frac{1}{2}}$
$C_s$	a constant $= (\sigma_s^2/\pi ck) [4\pi R/M_1]^{\frac{1}{2}}$
$e$	charge of electron
$f$	oscillator strength $= (1/\tau) (mc/8\pi^2 e^2) (g_2/g_1) \lambda_0^2$
$g_1, g_2$	statistical weights of normal and excited states
$\Delta H_{v,0}$	enthalpy of evaporation at $T_0$
$I_0$	incident intensity at wavenumber $\omega$
$I_\omega$	transmitted intensity at wavenumber $\omega$
$k$	Boltzmann's constant
$l$	optical path length
$L$	a constant $= (\Delta H_{v,0} - \Delta C_P T_0)/R$
$m$	mass of electron
$M_1, M_2$	masses of absorbing species and inert-gas species, respectively
$N$	concentration of absorbing species
$N_I$	concentration of inert gas
$P$	pressure of absorbing species
$P_I$	pressure of inert gas
$P_\omega$	absorption coefficient at $\omega$
$r$	$(\beta_{2,s}/\beta_{2,n})^2$
$R$	gas constant
$S$	integrated absorption

$$= \int_0^\infty P_\omega d\omega = \frac{\lambda_0^2}{8\pi c \tau} \frac{g_2}{g_1}$$

$T$	absolute temperature
$T_0$	reference temperature
$X$	$Nl$ = optical density
$\alpha$	$[(b_n + b_c)/b_D](\ln 2)^{\frac{1}{2}}$
$\beta$	total absorption
$\beta_1$	total absorption at low optical density
$\beta_2$	total absorption at high optical density
$\beta_{2,n}$	total absorption at high optical density considering only natural broadening
$\beta_{2,s}$	total absorption at high optical density considering both natural and self-broadening
$\delta$	Doppler broadening of an infinitesimal wavenumber band for an absorption line showing only dispersion broadening
$\lambda_0$	wavelength at center of absorption line
$\sigma_I^2$	optical collision cross section
$\sigma_s^2$	optical self-collision cross section
$\tau$	lifetime in excited state
$\Phi$	integration constant
$\omega$	wavenumber
$\omega_0$	wavenumber at center of absorption line

### ABSORPTION LAWS

The absorption measure used for this work was the total absorption,  $\beta$ , which is relatively independent of the resolution of the recording spectrometer<sup>1</sup>:

$$\beta = \int_0^\infty \frac{I_0 - I_\omega}{I_0} d\omega$$

$$\beta = \int_0^\infty [1 - \exp(-P_\omega X)] d\omega. \quad (1)$$

A schematic diagram of the equipment used for this work is shown in Fig. 1. The major components are the continuous-spectrum light source, the absorption cell, and the direct recording spectrometer. Auxiliary equipment consists of a temperature controlling and regulating furnace and a helium-dispensing unit by which the total pressure in the absorption cell is regulated. The details of the equipment are given in Appendix I.

If the absorbing gas is not electrically excited and the temperature is not too high, the absorption coefficient can be written<sup>2,3</sup> as follows:

$$P_\omega = \frac{Sb}{b_D} \frac{(\ln 2)^{\frac{1}{2}}}{\pi} \int_{-\infty}^{+\infty} \frac{\exp[-(\delta/b_D) \ln 2]^2}{(\omega - \omega_0 - \delta)^2 + b^2} d\delta. \quad (2)$$

This form describes the shape of the absorption line as a function of  $\omega$  for lines which show Doppler, natural, and collision broadening. It assumes a single absorption line without hyperfine structure, but since the line used in this study had hyperfine structure, the readings had to be corrected before further calculations could be made, as described in Appendix II.

It has been shown<sup>2,3</sup> that Eq. (1) can be integrated analytically in two limiting cases with the following results:

- (1) When  $P_\omega X$  is always small enough that

$$\exp(-P_\omega X) = 1 - P_\omega X,$$

then

$$\beta_1 = SX. \quad (3)$$

- (2) When the center of the absorption line is completely absorbed over a wavenumber range which is wide compared with the half-breadth of the absorption

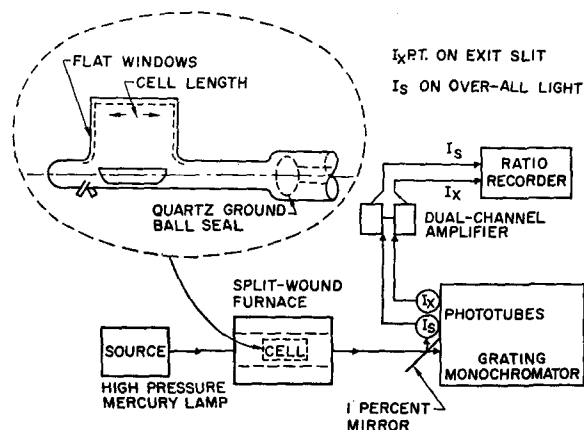


FIG. 1. Schematic diagram of equipment.

<sup>2</sup> A. C. S. Mitchell and M. W. Zemansky, *Resonance Radiation and Excited Atoms* (Cambridge University Press, Cambridge, England, 1961).

<sup>3</sup> S. S. Penner, *Quantitative Molecular Spectroscopy and Gas Emissivities* (Addison-Wesley Publishing Company, Inc., Reading, Massachusetts, 1959).

<sup>1</sup> R. Minkowski, *Z. Physik* 36, 839 (1926).

line, then

$$P_\omega = Sb/\pi(\omega - \omega_0)^2, \quad (4)$$

and

$$\beta_2 = 2(SbX)^{\frac{1}{2}}. \quad (5)$$

These limiting laws are apparent in Fig. 2, which is a dimensionless plot of

$$\beta(\ln 2)^{\frac{1}{2}}/2b_D \text{ versus } 6SX(\ln 2)^{\frac{1}{2}}/b_D$$

for various values of  $\alpha$ , the ratio of dispersion to Doppler broadening (curves of growth).

### METHOD

#### Determination of Optical Density and *f* Value

At this point let us suppose that measurements have been made in both the low- ( $\beta_1$ ) and high- ( $\beta_2$ ) density regions and that the low-density values have been extrapolated (dotted line in Fig. 2) into the high-density region. As an example, at a value of  $6SX(\ln 2)^{\frac{1}{2}}/b_D = 10^4$  and  $\alpha = 2$ , the value of  $\beta$  measured would correspond to Point 2 on Fig. 2. This is in the high-pressure region where the center of the line is fully absorbed ( $\beta_2$ ). Point 1 corresponds to a value of  $\beta$  that would be measured if the line were not fully absorbed at the center ( $\beta_1$ ). The ratio of the two values yields

$$\beta_1/\beta_2 = SX/2(SbX)^{\frac{1}{2}} = \frac{1}{2}(SX/b)^{\frac{1}{2}}. \quad (6)$$

Note that

$$S = \lambda_0^2 \frac{(g_2/g_1)}{(8\pi c\tau)}. \quad (7)$$

In the fully absorbed region the absorption is governed by the shape of the "wings" of the line. If for the moment we neglect collision broadening processes, then the half-breadth is controlled by the natural broadening<sup>2</sup>:

$$b = b_n = 1/(4\pi c\tau) \quad (8)$$

Then

$$\beta_1/\beta_2 = \frac{1}{2} \left[ (\lambda_0^2/2) (g_2/g_1) X \right]^{\frac{1}{2}}. \quad (9)$$

Introducing the ideal-gas law into the expression for optical density yields:

$$X = Nl = Pl/kT \quad (10)$$

and

$$\frac{\beta_1}{\beta_2} = \frac{1}{2} \left[ \frac{\lambda_0^2 g_2}{2 g_1 k T} \frac{l P}{k T} \right]^{\frac{1}{2}}. \quad (11)$$

The pressure is thus determined in terms of known constants or easily measured parameters. The problem is then reduced to a more familiar one, i.e., the determination of *f* value from absorption measurements on species of known optical density. The value of  $\tau$  is determined from Eqs. (5), (7), and (8) using measured

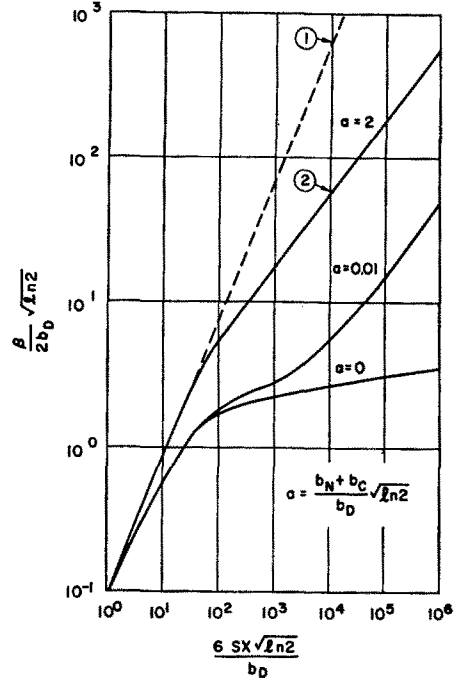


FIG. 2. Absorption versus optical density (curves of growth) for spectral lines with combined Doppler and dispersion broadening.

values of  $\beta_2$  and values of *X* calculated from Eq. (10). The *f* value is then calculated from the relationship

$$f\tau = mcg_2\lambda_0^2/8\pi^2e^2g_1. \quad (12)$$

#### Extrapolation of Absorption Measurements

In the previous section it was shown that *f* values and vapor pressures can be determined if absorption values can be extrapolated from low to high optical-density regions, or vice versa. Figure 2 suggests that absorption values could be plotted and extrapolated as a function of optical density or pressure. This cannot be done at this stage of the problem, however, because the pressure is not known, and presumably cannot be measured. But the temperature can easily be measured and the functional relationship between vapor pressure and temperature (Clapeyron equation) is known. In this section the Clapeyron equation is introduced into the absorption equations (3) and (5) to yield a relationship between the total absorption ( $\beta_1$  or  $\beta_2$ ) and temperature that can be extrapolated.

The Clapeyron relationship between temperature and vapor pressure above a pure liquid can be written

$$\ln P = -L/T + B \ln T + \Phi, \quad (13)$$

where  $L = (\Delta H_{v,0} - \Delta C_P T_0)/R$ ,  $\Delta H_{v,0}$  is the enthalpy of evaporation at reference temperature  $T_0$ ,  $B = \Delta C_P/R$ , and  $\Phi$  is a constant of integration.

In the region of low optical density, represented by Eq. (3), the relationship between absorption and

pressure (assuming gas ideality) is

$$\beta_1 = SX = SlN = SlP/kT. \quad (14)$$

Taking the logarithm of Eq. (14), combining with Eq. (13), and rearranging terms yields

$$\ln[\beta_1 T^{(1-B)}] = -L/T + \ln(Sl/k) + \Phi. \quad (15)$$

Since all the terms in Eq. (15) are constant except  $\beta_1$  and  $T$ , it can be seen that a plot of  $\ln[\beta_1 T^{(1-B)}]$  versus  $T^{-1}$  will be linear. This relationship allows a linear least-squares line to be fitted to the data and thus allows the absorption values to be extrapolated.

A similar treatment in the fully absorbed region ( $\beta_2$ ) yields

$$\ln[\beta_2 T^{(4)(1-B)}] = -L/2T + \frac{1}{2}\Phi + \frac{1}{2}\ln[(4Sbl)/k]. \quad (16)$$

This equation shows that a linear relationship will exist between  $\ln[\beta_2 T^{(4)(1-B)}]$  and  $T^{-1}$  if all the rest of the parameters remain constant. The dispersion half-breadth  $b$  is in general not a constant. If natural broadening dominates, i.e., if there is no foreign gas present and self-broadening is insignificant, then  $b$  will be constant and Eq. (16) would represent a valid extrapolation. If self-broadening is significant,  $b$  will vary with the temperature as well as the pressure of the absorbing species. The problem of extrapolating data under these conditions is treated in the next section.

In the case where a foreign gas is present,  $b$  will not be constant. However, if the pressure of the inert gas is increased sufficiently, the collision broadening can be made the dominant dispersion broadening process. The collision half-breadth,  $b_c$ , varies with temperature and inert gas pressure,  $P_I$ . Equation (16) cannot be used, but a new expression can be developed as follows:

$$b = b_n + b_s + b_c \sim b_c, \\ b_c = (\sigma_I^2 N_1 / \pi c) [2\pi R T (1/M_1 + 1/M_2)]^{1/2}.$$

Applying the ideal-gas law,

$$b_c = C_I P_I / T^{1/2}$$

where

$$C_I = (\sigma_I^2 / \pi c k) [2\pi R (1/M_1 + 1/M_2)]^{1/2}.$$

From Eq. (5) and the ideal-gas law,

$$\beta_2 = [4SC_I P_I l P / k T^{3/2}]. \quad (17)$$

Combining Eq. (17) with the Clapeyron equation as before yields

$$\ln[\beta_2 T^{(4)(3-2B)}] = -L/2T + \frac{1}{2}\Phi + \frac{1}{2}\ln[(4SP_I C_I l)/k]. \quad (18)$$

With a constant inert gas pressure, a plot of  $\ln[\beta_2 T^{(4)(3-2B)}]$  versus  $T^{-1}$  is linear with slope  $-L/2$ .

This allows extrapolation and also the determination of the constant  $L$ , which is related to the enthalpy of evaporation [Eq. (13)].

### Correction for Self-Broadening

In the absence of an inert gas, the effect of self-broadening can be accounted for if the value of  $L$  is known. Subtracting the self-broadening contribution from the absorption measurements would reduce the problem to one in which the only dispersion broadening is natural broadening. This problem has been solved previously.

Assume that we have made an absorption measurement with just the absorbing species present at a high enough pressure to put us in the square-root absorption law region.  $\beta_{2,s}$  is the measured absorption with self-broadening present.  $\beta_{2,n}$  is the absorption that would have been observed if no self-broadening were present. Let

$$r = [\beta_{2,s} / \beta_{2,n}]^2, \quad (19)$$

$$r = [4S(b_s + b_n)X / 4Sb_n X] = 1 + (b_s / b_n), \quad (20)$$

where  $b_s$  is the self-collision half-breadth

$$b_s = \sigma_s^2 (N / \pi c) [(4\pi R T / M_1)]^{1/2} \quad (21)$$

Substituting Eq. (21) into (20), introducing the ideal-gas law, and combining with Eq. (13) yields

$$\ln[(r-1)T^{(4-B)}] = -L/T + \Phi + \ln(C_s / b_n), \quad (22)$$

where

$$C_s = (\sigma_s^2 / \pi c k) (4\pi R / M_1)^{1/2}. \quad (23)$$

From Eq. (16) the natural broadening contribution to the absorption is

$$\ln[\beta_{2,n} T^{(4)(1-B)}] = -L/2T + \frac{1}{2}\Phi + \frac{1}{2}\ln[(4Sb_n l)/k]. \quad (24)$$

In Eq. (24) the terms  $\frac{1}{2}\Phi + \frac{1}{2}\ln[(4Sb_n l)/k]$  are constant, but unknown at this point. The same is true of  $\Phi + \ln(C_s / b_n)$  in Eq. (22).  $T$  and  $\beta_{2,s}$  are measured quantities. We assume that  $L$  has been determined by previous absorption measurements with added inert gas and that  $B$  is known. Values of  $\beta_{2,n}$  can then be derived from  $\beta_{2,s}$  values by using Eqs. (19), (22), and (24) as follows:

- (1) A value  $\frac{1}{2}\Phi + \frac{1}{2}\ln[(4Sb_n l)/k]$  is guessed.
- (2) A value of  $\beta_{2,n}$  is calculated for each value of  $T$  at which a data point exists using Eq. (24).
- (3) A value of  $r$  is calculated for each data point [Eq. (19)] using measured values of  $\beta_{2,s}$  and values of  $\beta_{2,n}$  calculated above.
- (4) A least-squares line is solved for in the linear relationship between  $\ln[(r-1)T^{(4-B)}]$  versus  $1/T$  [Eq. (22)].
- (5) If the slope of the line is not  $-L$ , as it should be, a new value of  $\frac{1}{2}\Phi + \frac{1}{2}\ln[(4Sb_n l)/k]$  is guessed.

When a satisfactory set of values is found,  $\beta_{2,n}$  will be known for each data point. The problem is then reduced to the one first discussed, i.e., the determination of *f* value and pressure from absorption measurements in which the dispersion breadth is solely due to natural broadening. When the pressures and *f* value (and  $\tau$ ) have been determined, a value of the optical self-collision cross section ( $\sigma_s^2$ ) can be calculated using Eqs. (8), (20), (21), and the ideal-gas law.

**MEASUREMENTS**

Optical absorption measurements of the bismuth 3067-Å line were made over a temperature range of 780° to 1280°K. These measurements were used to calculate a vapor pressure of monatomic bismuth, the lifetime in the excited state of the bismuth 3067-Å line, the collision cross sections of the absorption vapors with helium, and the self-collision cross sections.

The actual measurement of the total absorption was the area of absorption,  $A/I_0$ , in square inches divided by the incident intensity in arbitrary chart units. This is related to the total absorption  $\beta_1$  by an instrumental constant which depends on the scanning rate of the spectrometer and the original units of the measurement.

**Bismuth 3067-Å Line**

Figure 3 shows the raw bismuth 3067-Å absorption data of the whole range of measurements. The absorptions in the region  $10^3/T > 1.25$  are in the low-pressure linear-absorption area. The higher temperatures,

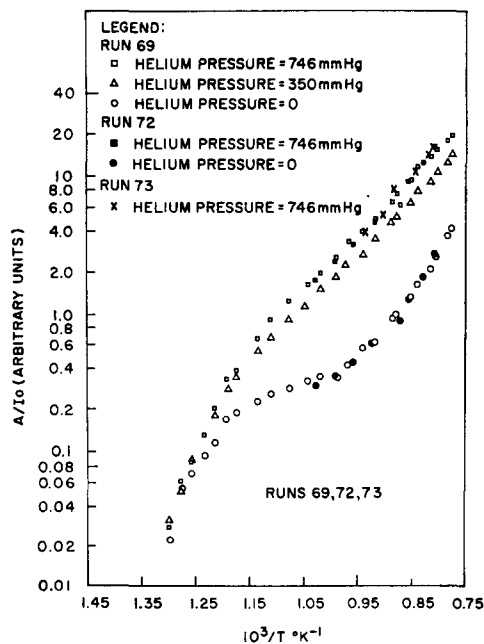


FIG. 3. Uncorrected optical absorption versus inverse temperature for Bi 3067-Å line for various helium pressures.

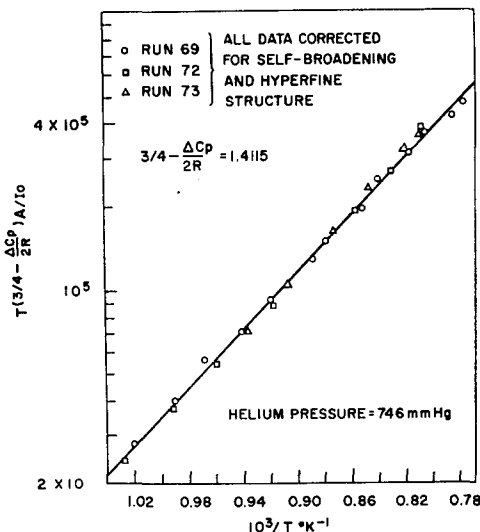


FIG. 4. Optical absorption versus inverse temperature for Bi 3067-Å line, with helium pressure of 746 mm Hg, corrected for self-broadening and hyperfine structure.

$10^3/T < 1.05$ , are in the absorption region where the center of the line is fully absorbed. The measurements with helium added show higher absorption than the pure bismuth experiments. The slope of the lines is also interesting. The slope of both lines with added helium is essentially the same. Collision broadening is the dominant broadening process over this range and is constant for any one helium pressure. The pure-bismuth run shows increasing slope at higher temperatures, i.e., higher pressures. This is caused by increasing self-broadening as the pressure increases.

The lines were corrected for hyperfine structure using the correction chart in Appendix II. A value of the constant *L* was determined from the collision-broadened values plotted in Fig. 4. This was then used to correct the zero helium pressure values for self-broadening. It should be noted that the self-collision cross sections include not only the monatomic bismuth interactions but also the interactions of monatomic and diatomic bismuth vapor species. The resulting vapor pressure equation is:

$$\log_{10} P = -(10\,521/T) + 9.5380 - 1.323 \log_{10} T,$$

where *P* is the pressure of the bismuth species in atmospheres and *T* is the temperature in degrees Kelvin. A representative value of the vapor pressure at 1000°K with estimated confidence limits is compared in Table I with the corresponding values of Yoshiyama,<sup>4</sup> Brackett and Brewer,<sup>5</sup> and Aldred and Pratt.<sup>6</sup> A value of vapor pressure calculated from the enthalpy of evaporation and heat capacities (from

<sup>4</sup> S. Yoshiyama, J. Chem. Soc. Japan **62**, 8, 204 (1941).  
<sup>5</sup> E. Brackett and L. Brewer, University of California Radiation Laboratory Report UCRL 3712, March 1957.  
<sup>6</sup> A. T. Aldred and J. N. Pratt, J. Chem. Phys. **38**, 1085 (1963).

TABLE I. Vapor pressure of monatomic bismuth at 1000°K.

This work	+0.7
	1.1 $\times 10^{-5}$ atm -0.5
Bracket and Brewer <sup>a</sup>	+1.3
	2.1 $\times 10^{-5}$ atm -0.8
Yoshiyama <sup>b</sup>	1.35 $\times 10^{-5}$ atm
Aldred and Pratt <sup>c</sup>	1.38 $\times 10^{-5}$ atm
Third-law method (this work)	+1.3
	1.8 $\times 10^{-5}$ atm -0.7

<sup>a</sup> See Ref. 5.<sup>b</sup> See Ref. 6.<sup>c</sup> See Ref. 10.

Stull and Sinke<sup>7</sup>) using the third-law method<sup>8</sup> is included.

Brackett and Brewer's value is 88% higher than the value calculated from the absorption data. However, the uncertainty in both values is large enough that they overlap. Yoshiyama's measurements were made in the temperature range 912° to 962°K using a torsion effusion cell. His results agree well with the optical absorption data if the slope of the Clapeyron plot of Yoshiyama's data is made to agree with the value obtained from the present absorption work in order to extrapolate his values to 1000°K. The lifetime,  $f$  values, and collision cross sections are listed in Table II with their estimated 95% confidence limits.

No  $f$  values or collision cross sections were found in the literature for the bismuth 3067-Å line, so no direct comparisons could be made.

### DISCUSSION

The method outlined in the previous sections has obvious application in the determination of  $f$  values for elements or compounds whose vapor pressure is not known. It is especially useful for materials, such as bismuth, having more than one vapor species. In this case simple weight-loss measurements for pressure determination cannot be applied. Optical absorption techniques can measure the vapor pressures of each of the species independently. Even if vapor pressures have been determined, the method described provides a consistency check.

The measurements described in the previous section seem to yield reasonable results for the vapor pressure of bismuth. It is unfortunate that no  $f$  values are available for direct comparison. In the method described, however, the two are determined simultaneously. Agreement of measured pressure values with the results of others, and the internal consistency with

third-law values lends credence to the quoted  $f$  values.

There are limitations on the application of this method. The species must be present over a concentration range large enough to allow measurements to be made in the fully absorbed ( $\beta_2$ ) and non fully absorbed ( $\beta_1$ ) regions. Optical paths can be increased to allow for low densities, but this too has limits. Another drawback is the need for a transparent container. This limits the temperature to about 1100°C for quartz cells and excludes some reactive species. Sapphire windows in metallic cells can be used to extend the range somewhat, but only by a few hundred degrees. One solution to these difficulties might be to use a technique demonstrated by Vidale.<sup>9</sup> He used cells of refractory metals with small holes in the ends. The windows in the furnace system were far removed from the refractory metal cells and could thus be kept cold. Light was passed through the holes in the cell for the absorption determination. Because of the diffusion or streaming of the gas from these holes, the total absorption path is difficult to determine, which limits the accuracy of the method. Another technique for eliminating the windows involves absorption measurements on vapors effusing into a vacuum from a Knudsen cell.<sup>10</sup> The vapor density is low, but the optical path can be increased by reflecting the light beam back and forth with mirrors. Even with this arrangement it is difficult to get the wide range of optical densities needed for the use of the method described.

### SUMMARY

A method for determining  $f$  values and vapor pressures solely by optical absorption techniques has been demonstrated. Measurements on the bismuth 3067-Å line using this technique seem to be in good agreement with other measured values of vapor pressure.

### APPENDIX I. EQUIPMENT

The major components of the equipment (Fig. 1) are the continuous-spectrum light source, the absorption cell, and the direct recording spectrometer.

TABLE II. Bismuth spectroscopic quantities (3067-Å line).

$\tau$	+2.3
	5.4 $\times 10^{-9}$ sec -1.7
$f$	+0.061
	0.131 -0.039
$\sigma_s^2$	+3000
	3100 Å <sup>2</sup> -1000
$\sigma_{Ho}^2$	+12.2
	25.3 Å <sup>2</sup> -8.5

<sup>7</sup> D. R. Stull and G. C. Sinke, *Thermodynamic Properties of the Elements* (American Chemical Society, Washington, D.C., 1956).<sup>8</sup> G. N. Lewis and M. Randall, revised by K. S. Pitzer and L. Brewer *Thermodynamics* (McGraw-Hill Book Company, Inc., New York, 1961).<sup>9</sup> G. L. Vidale, Space Sciences Laboratory, General Electric Company, Report R60SD330 (1960).<sup>10</sup> G. D. Bell, M. H. Davis, R. B. King, and P. M. Routly, *Astrophys. J.* **127**, 775 (1958).

The light source used to supply a continuum in the desired frequency range was a high-pressure mercury lamp, H3FE, manufactured by the General Electric Company. The lamp was contained in a water-cooled jacket and the power input was stabilized by two ballast transformers. The maximum fluctuation of the light intensity was not greater than 2%. The lamp emitted an approximately continuous intensity over the wavelength region from 2600 to 4000 Å except in the vicinity of mercury emission lines. The cell used for the absorption measurements was made entirely of quartz with optically flat, polished windows. Quartz cells were obtained from the Euclid Glass Engineering Laboratory, Cleveland, Ohio, and the Superior Glass Apparatus Company, Ann Arbor, Michigan. The window spacing employed for this work was 4.6 cm.

The furnace used to heat the quartz cell was a split-wound resistance furnace. The furnace had two main windings and two end windings, separately controlled to offset the effect of end cooling. By regulating the power input to the various windings, it was possible to control the temperature in the immediate vicinity of the cell to  $\pm 2^\circ\text{C}$ . The necessary isothermal volume in the furnace was a cylinder 5 cm in diameter and 10 cm in length. The absorption cell proper and a small crucible containing the absorbing material were located in the center of this isothermal range. Temperatures were measured in four different positions along the cylinder with calibrated Chromel-Alumel thermocouples were placed in the immediate vicinity of the cell.

The total pressure in the absorption cell was regulated by a helium dispensing unit. High-purity helium was slowly released from a high-pressure cylinder through a liquid-nitrogen cold trap into the vacuum line. The quartz-to-quartz seal in the absorption cell served the dual purpose of containing the absorbing atoms while allowing the helium atoms to pass back and forth quite freely. The seal worked remarkably well, allowing almost instantaneous changes of helium pressure in the cell proper while keeping the rate of diffusion of the absorbing atoms from the cell to less than one thousandth that of the evaporation rate estimated from kinetic theory. The helium pressure in the system was measured by a mercury manometer.

A plano-convex lens was placed at its focal distance from the mercury lamp source to give a parallel beam of light through the absorption cell. After passage through the cell, the light was condensed with another plano-convex lens before it reached the spectrometer. The mercury lamp source was not a point source, and hence some divergence was still present. This did not affect the measurements, however, since the path length through the cell was less than 5 cm. In this length the beam of light was essentially parallel. The absorbed radiation was analyzed by means of a Leeds and Northrup spectrochemical analyzer containing a small plane grating monochromator. The spectrometer

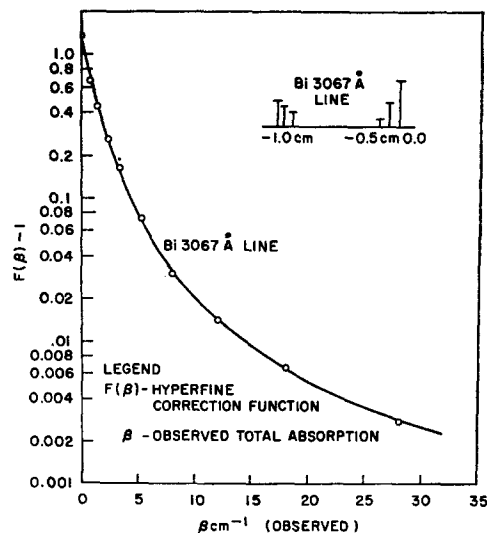


FIG. 5. Hyperfine structure correction chart for Bi 3067-Å line.

is 30 in. long and is equipped with a 3-in.-wide grating with 30 000 lines per inch. Spectra were obtained which demonstrated a second-order resolution of 0.1 Å in the visible and ultraviolet regions.

Approximately 1% of the light through the cell was reflected by a mirror in front of the entrance slit to a reference phototube called  $I_s$ . The remaining radiation passed through the spectrograph and was recorded by the phototube  $I_x$ , which was at the exit slit. The radiation striking the  $I_s$  tube had wavelengths from approximately 2500 to 4000 Å. The light striking the  $I_x$  phototube corresponded to radiation in a small wavelength region.

The signals from the two phototubes were fed into a dual-channel amplifier. The power input to the phototubes could be adjusted to balance the intensity of the two signals in the amplifier at any particular reading. The output from the dual-channel amplifier was recorded on a ratio recorder, which displayed the intensity ratio  $I_x/I_s$  as a function of wavelength. Splitting the radiation before it entered the monochromator helped stabilize the recorded intensity trace. The instrument was set to scan in a particular wavelength region at a speed of 2.9 Å/min.

## APPENDIX II. HYPERFINE STRUCTURE

Many atomic transitions, including the ones corresponding to the bismuth 3067-Å absorption line discussed here, have a hyperfine structure. The hyperfine structure has an effect on the observed total absorption of an atomic absorption line when total absorption is not proportional to  $SX$  or when the hyperfine components of the line do not completely overlap.

To evaluate the effect of hyperfine structure on an absorption line, an expression for the absorption coefficient that accounts for absorption by each hyperfine

component must be substituted into the expression for the total absorption. The bismuth 3067-Å line has six hyperfine components spread over a distance of 1.06 cm<sup>-1</sup>. The spacings and relative strengths of the components of this line are shown in Fig. 5.

The absorption coefficient for an absorption line made up of hyperfine components, each of which follows the square-root absorption law [ $\beta_2 = 2(SbX)^{\frac{1}{2}}$ ] and has its center at a particular  $\omega_{0i}$ , is written as

$$P_{\omega} = (Sb/X) \sum X_i / (\omega + \omega_{0i})^2, \quad (25)$$

where  $X_i$  is the optical density associated with Hyperfine Component  $i$ . This coefficient can be introduced into the expression for the total absorption  $\beta$  and the integral divided by the expression for the total absorption in the square-root region that would be obtained if there were no hyperfine structure. The resultant expression, shown below, represents a correction factor which can be applied to absorption data taken in concentration regions where the total absorption is

proportional to the square root of the optical density (high pressure):

$$F(\beta) = \frac{1}{\beta_{NH}} \int_0^{\infty} [1 - \exp(-P_{\omega}X)] d\omega, \quad (26)$$

where  $\beta_{NH}$  equals the total absorption that would be obtained if no hyperfine structure were present. Observed values of absorption ( $A/I_0$ ) or  $\beta$  are corrected by dividing by  $F(\beta)$ .

This integral has been evaluated numerically as a function of  $\beta_{NH}$  for the hyperfine structures of the bismuth 3067-A line using an IBM 709 computer. The resulting values of  $F(\beta)$  are plotted as a function of  $\beta$  (the observed total absorption) in Fig. 5. The limits of complete separation of the hyperfine components can be calculated<sup>4</sup> from

$$\sum_{i=1}^n X_i^{\frac{1}{2}} / (\sum X_i)^{\frac{1}{2}}$$

and are shown also on the graph.

## Pulse Radiolysis Studies. VII. The Absorption Spectra and Radiation Chemical Yields of the Solvated Electron in the Aliphatic Alcohols\*

MYRAN C. SAUER, JR., SHIGEYOSHI ARAI,† AND LEON M. DORFMAN

Chemistry Division, Argonne National Laboratory, Argonne, Illinois

(Received 23 September 1964)

The absorption spectra of the solvated electron in five aliphatic alcohols have been determined by the pulse radiolysis method. For the alcohols: ethylene glycol, methanol, ethanol, *n*-propanol, and isopropanol, the absorption maxima show a red shift with decrease in the value of the static dielectric constant. The absorption maxima for these alcohols are, respectively, 5800, 6300, 7000, 7400, and 8200 Å. The molar extinction coefficient at the maximum and the oscillator strength of the broad absorption band has been determined for each alcohol.

The radiation chemical yields of the solvated electron in these irradiated alcohols as determined by pulse radiolysis are, respectively, 1.2, 1.1, 1.0, 1.0, and 1.0 per 100 eV.

The correlation between the transition energy for optical excitation of the solvated electron and the dielectric behavior of the liquid is discussed in terms of the theory.

### INTRODUCTION

**A** KNOWLEDGE of the properties of the solvated electron is of interest in a number of areas of physical science. These range from radiation chemical kinetics, where its intrinsic importance lies in its role as a primary species, to that branch of spectroscopy which deals with small ions and with the electron in polar liquids, and ultimately to the subject of the structure of liquids.

The occurrence of electron solvation in the aliphatic

alcohols has recently been established<sup>1-4</sup> and the absorption spectra reported for ethanol<sup>1,2,4</sup> and methanol.<sup>3</sup> The alcohols represent an interesting series of liquids for which the optical absorption spectrum of the bound electron may be examined as a function of the dielectric constant, a fundamental parameter of the theory<sup>5-7</sup>

<sup>1</sup> I. A. Taub, M. C. Sauer, Jr., and L. M. Dorfman, *Discussions Faraday Soc.* **36**, 206 (1963).

<sup>2</sup> I. A. Taub, D. A. Harter, M. C. Sauer, Jr., and L. M. Dorfman, *J. Chem. Phys.* **41**, 979 (1964).

<sup>3</sup> G. E. Adams, J. H. Baxendale, and J. W. Boag, *Proc. Roy. Soc. (London)* **A277**, 549 (1964).

<sup>4</sup> L. I. Grossweiner, E. F. Zwicker, and G. W. Swenson, *Science* **141**, 1180 (1963).

<sup>5</sup> A. C. Davydov, *Zh. Eksperim. i Teor. Fiz.* **18**, 913 (1948).

<sup>6</sup> R. Platzman and J. Franck, *Z. Physik* **138**, 411 (1954).

<sup>7</sup> J. Jortner, *Radiation Res. Suppl.* **4**, 24 (1964).

\* Based on work performed under the auspices of the U.S. Atomic Energy Commission.

† Permanent address: Department of Physical Chemistry, Tokyo Institute of Technology, Tokyo.